Environmental Science Advances

ROYAL SOCIETY OF CHEMISTRY

PAPER

View Article Online
View Journal | View Issue

Cite this: *Environ. Sci.: Adv.*, 2026, **5**, 1070

High resolution porewater profiling of methylmercury with a novel equilibrium passive sampler

Jada C. Damond, [a] Cynthia C. Gilmour [b] and Upal Ghosh *[a]

Accurate quantification of sediment porewater methylmercury (MeHg) profiles is critical for understanding Hg fate, transport, and informing remediation design, yet direct porewater profiling remains challenging. Equilibrium-based passive samplers (EqPS) offer an alternative, providing fine-scale, time-integrated measurements and convenience. In this study, we deployed an EqPS consisting of activated carbon suspended in agarose gel (ag+AC) in estuarine and freshwater sediment microcosms to obtain porewater MeHg profiles at 0.5 cm vertical resolution. Our objectives were to evaluate whether ag+AC samplers could reproduce porewater MeHg profile shapes and concentrations across redox gradients and contrasting geochemical conditions. Following 4 week deployments across the sediment–water interface ag+AC samplers produced distinct depth profiles that corresponded closely with directly measured porewater profiles and exhibited maxima at redox transition zones where net methylation is most likely. Using a previously derived equilibrium partition coefficient ($10^{2.96}$ L kg^{-1}) ag+AC samplers predicted, on average, directly measured porewater MeHg concentrations to within a factor of about two. Across both sediment types, porewater MeHg alone explained ~65% of the variability in passive sampler MeHg despite wide ranges in DOC, sulfide, iron, and salinity. These results demonstrate ag+AC EqPS can provide fine-scale porewater MeHg profiles and accurate concentration estimates across diverse sedimentary environments.

Received 24th December 2025
Accepted 17th February 2026

DOI: 10.1039/d5va00492f

rsc.li/esadvances

Environmental significance

Accurate spatial quantification of porewater methylmercury (MeHg) is critical for understanding mercury fate and transport, bioaccumulation, and for informing remediation design. However, direct extraction and measurement is challenging. In this research, we deployed an equilibrium passive sampler consisting of activated carbon suspended in agarose gel sheet in estuarine and freshwater sediment microcosms to obtain porewater MeHg profiles at 0.5 cm vertical resolution. Passive sampler derived profiles identified depth-resolved MeHg concentrations that corresponded with directly measured profiles and with redox transition zones where net methylation is most likely to occur. Identifying the depth of the methylation zone can inform targeted remediation strategies and improve assessments of benthic exposure risk.

1 Introduction

Mercury (Hg) is a global pollutant that is responsible for fish consumption advisories worldwide. Dealing with mercury as a pollutant in aquatic environments poses complex challenges, because of its biogeochemical transformations. Site assessment and remediation require an understanding of mercury and methylmercury (MeHg) exposure to the food web and ultimately to humans.

Sediments are an important location of net MeHg production in many ecosystems. Mercury in sediments is methylated to MeHg by anaerobic microbes – often sulfate or iron reducing bacteria – at a depth beneath the sediment where redox chemistry is conducive to their microbial activity.[1,2] Consequently, MeHg concentrations in sediments ($[MeHg]_{sed}$) and porewaters ($[MeHg]_{PW}$) vary spatially within the sediment.[3] Because Hg methylation is controlled by microbial activity, sediment biogeochemistry impacts the shape and magnitude of the vertical porewater MeHg depth profile. The ability to capture these profiles can elucidate how MeHg forms and transports in sediment systems. High resolution porewater profiling allows an accurate calculation of diffusive flux within the sediment column and across the sediment–water interface. Porewater concentrations provide valuable information for evaluating the performance of a remedial cap for which the aim is to decrease porewater MeHg in the surface sediments.[4,5]

[a]*Department of Chemical, Biochemical, and Environmental Engineering, University of Maryland Baltimore County, Baltimore, MD 21250, USA. E-mail: ughosh@umbc.edu*
[b]*Smithsonian Environmental Research Center, 647 Contees Wharf Road, Edgewater, MD 21037, USA*

Porewater MeHg profiles are also critical to understanding bioaccumulation within epibenthic organisms. Several studies show that MeHg exposure to epibenthic organisms is best quantified in the top sediments, and vertical profiling is useful for understanding benthos bio-uptake.[6,7] Further, bioturbation by benthic organisms may impact MeHg concentrations by physical disturbance[8] and oxidation in the top sediment layer (as postulated in Sanders, 2018).[9]

Though porewater profiles are incredibly valuable, they are difficult to retrieve with traditional sampling methods that include removal of intact sediment cores, sectioning of the cores, and extraction of porewater within sections. Extracting porewater from collected sediment cores is expensive and laborious, as it requires handling in an anaerobic glovebox in the field to preserve redox conditions and prevent oxidation of metal species and degradation/precipitation of aqueous MeHg.[10] The method also is limited by the small volumes of extractable porewater from thin sections of sediment cores. Another method of sediment porewater sampling by syringe extraction introduces uncertainty of sampling depth and zone of collection which can also be impacted by entrained surface water.[3]

Fine-scale vertical MeHg profiling using kinetic-based samplers (*i.e.* diffusive gradient in thin films, DGTs) have been advantageous for studying Hg dynamics.[11–13] However, researchers have encountered difficulty with their interpretations due to porewater depletion by the samplers and variation of diffusion coefficients between sites.[11,12] Particularly, the presence of dissolved organic matter (DOM) significantly impacts MeHg and Hg diffusion rates into the sampler for which the estimated aqueous concentrations are based on.[12,14,15] MeHg will complex to DOM of varying character and sizes, leading to a wide range of diffusion rates.[16] The biogeochemical impacts on the diffusion rate warrants the need for site-specific calibration when using DGTs. These concerns have hindered its acceptance in regulatory practice.[17]

A novel equilibrium-based MeHg passive sampling method has been developed[18,19] as a novel approach to bypass these difficulties seen with kinetic-based sampling. The equilibrium passive sampler explored in this study is made of powdered activated carbon embedded in an agarose polymer sheet (ag+AC). Investigations[18] found that sampling was kinetically influenced by MeHg interactions with AC particles and not limited by diffusion through the gel for this material. AC exhibited relatively rapid desorption of Hg and MeHg, indicating that this sorbent is capable of reversible, equilibrium measurements. Washburn *et al.*[19] showed that the experimentally determined sampler–water partitioning coefficient (K_{PS}) values for MeHg complexed with a variety of natural organic matter (MeHgNOM) and small thiols are about 10^3 L kg^{-1} and have provided reasonably good $[MeHg]_{PW}$ estimations in slightly sulfidic sediments where MeHg sulfides could be important species. Sampler equilibration time in sediments was approximately 1 to 2 weeks. In sediment–water microcosms,[19] porewater concentrations estimated with isotherm-calibrated passive samplers agreed within a factor of 2 to 4 with directly measured concentrations demonstrating a potential new approach to passive sampling of MeHg. These microcosms also demonstrated that a single ag+AC passive sampler sheet placed across the sediment–water interface provided both porewater and overlying water measurements, revealing the potential for it to capture the critical measurement of gradients across the sediment interface.

In this study, we evaluated the ability of the ag+AC passive samplers (PS) to adequately resolve porewater MeHg profiles at 0.5 cm resolution. Because the PS could be formed into a desired size thin sheet, we were able to deploy an adequate size sampler above and within sediments to capture aqueous MeHg concentrations both in the surface water and depth dependent concentrations within the sediments. Samplers were deployed in freshwater and estuarine-sourced sediment microcosms to study their applicability in two geochemically different types of environments. Samplers were deployed within sediment microcosms to span a depth range sufficient to capture the MeHg maxima associated with the MeHg production zone. Samplers were deployed for a month in pre-equilibrated microcosms. Freshly constructed sediment–water microcosms often exhibit a pulse of microbial activity and net MeHg production due to disturbance.[20] Pre-equilibration allows most of the pulse to pass. The PS deployment time frame was chosen based on the measured equilibration time for the samplers. We compared PS-derived MeHg profiles (0.5 cm resolution) to profiles obtained by direct porewater measurements made at a 1 cm resolution at the end of the PS deployment.

2 Methods

2.1 ag+AC passive sampler synthesis

The ag+AC polymer material was synthesized as described in Washburn *et al.*[19] Briefly, virgin AC derived from bituminous coal (Calgon Type 3055; 80 × 325 TOG LF) was sieved to >53 μm, then washed with deionized (DI) water and allowed to dry in a 30 °C oven prior to casting within gels to ensure uniformity. This AC was embedded in a 1.5 wt% agarose gel to make a polymer embedded with 1.5 wt% AC. To make the polymer, 20 mL DI was added to 0.3 g agarose powder (low EEO) and 0.3 g AC. This suspension was stirred, *via* a magnetic stir bar, in a boiling water bath for 4.5 minutes, after which the solution was cast between two glass plates separated by a 1 mm spacer. After cooling, the formed gelatinous polymers were cut into 4 cm by 8 cm segments (SI Fig. S1) to serve as passive samplers (referred to as 'PS' or simply 'samplers' throughout this document). Samplers were designed to capture depth profiles up to 8 cm, with approximately 1 cm exposed to the overlying water and the remaining 7 cm embedded in the sediment. PS polymers were sandwiched in polypropylene mesh (McMaster-Carr 69 × 69 mesh) to provide protection and rigidity. The protective mesh was soaked in a 10% HCl solution overnight then rinsed with DI water prior to PS enclosure. Prior to deployment, enmeshed PS were deoxygenated in DI with N_2 gas for over 30 min to minimize oxygen input into the sediment.

2.2 Sediment microcosm set-up

Sediment mixes were made up to represent two environmental conditions, freshwater and estuarine sediments, to evaluate PS

performance in different biogeochemical environments. To provide both elevated Hg concentration and fresh organic matter for MeHg production, we mixed freshly collected sediments and soils at mid-Atlantic regional background Hg levels with Hg-contaminated soil collected for prior experiments from the Berry's Creek Study Area (BCSA) in New Jersey, USA.[20]

The estuarine sediment mix comprised intertidal surface marsh soils from the BCSA[20] mixed with intertidal marsh soil from a mesohaline marsh (Global Change Research Wetland, GCREW) at the Smithsonian Environmental Research Center (SERC) in Maryland, USA.[21] The freshwater sediment mixture also contained marsh soil from BCSA, mixed with sediment collected from a freshwater pond in Watershed 101 on the SERC campus.[22] Detailed descriptions of sampling sites and mixtures are in Table S2.

The contaminated sediment/soil was diluted with sediment at background levels to yield a sufficient volume for this study. A target Hg concentration range between 1 and 10 μg gdw^{-1} was set to be high enough to be considered contaminated, and to obtain detectable direct porewater measurements to aid in passive sampler performance assessment. Final values are shown in Table 1. To make up the sediment mixes, large detritus was removed, and soils were sieved to 2 mm. Sieved soils were homogenized with a food processor to minimize variability between replicate microcosms. Sediment mixtures were homogenized with a paint mixer immediately prior to microcosm construction, after which they are referred to as sediment throughout this document. The additional processing will influence sediment dynamics in a way that is not representative of field conditions and is not recommended or needed for field measurements. However, for the sampler development effort in the present study, sediment homogenization was performed to minimize sampler variability between microcosms replicates.

Oligohaline conditions were targeted for the estuarine microcosms. Surface water from the GCREW intertidal marsh (SERC), which measured 8 ppt with a refractometer, was diluted by half with DI water, yielding an initial salinity of 4 ppt in the overlying water. The freshwater microcosms were topped with freshwater from SERC Watershed 101, which had a salinity of 0 ppt, taken just below the sampled pond.

Microcosms were housed in opaque 7.6 L HDPE buckets (SI Fig. S2 and S3). The homogenized sediment mixtures were added to a depth of 10 cm and then topped carefully with 3 L of overlying water. For the duration of the experiment, overlying water in both microcosms was aerated by pumping air through a clean air stone. The microcosms were loosely capped.

Microcosms were equilibrated for two weeks prior to insertion of passive samplers to allow re-development of redox gradients after mixing. The choice of two weeks was based on prior microcosm studies that used similar sediments.[18–20,23] Detailed time course measurements of biogeochemical conditions in these prior studies often showed strong pulse of net MeHg production, probably due to sediment processing. Two-week equilibration generally allows the peak of this production to pass, providing more stable MeHg concentrations during passive sampler exposures. To monitor conditions in the microcosms, porewater ORP was measured using an InLab Redox Micro probe (Mettler Toledo) to determine the depth to anoxia (ORP < 0 mV). After one week anoxia was observed at 3.2 cm and 2.5 cm below the SWI of the freshwater and estuarine microcosms, respectively.

Two weeks after construction, the 4 by 8 cm passive samplers in their protective mesh were then inserted and remained in place for 4 weeks before microcosm deconstruction. The deployment timeframe was selected based on results from a study investigating kinetic uptake of MeHg complexed with DOM into the PS.[19] We followed surface water chemistry approximately bi-weekly, including oxidation–reduction potential, NH_4, and salinity (SI Table S3). The surface water was replenished with source water every two weeks to best preserve the steep redox gradients that would be found in a natural

Table 1 Initial measurements in overlying water, porewater, and sediments

Initial measurements in overlying water (ow) & porewater (pw)								
Sediment type	Matrix	SO_4^{2-} (mM)	Cl^- (mM)	DOC (mg L^{-1})	pH	S^{2-} (μM)	MeHg (ng L^{-1})	THg (ng L^{-1})
Estuarine	ow	1.6 ± 0.6	29.1 ± 5.4	2.4 ± 0.2	7.4 ± 0.1	0.46 ± 0.03	BDL	nm
	pw	4.5 ± 1.6	126.8 ± 26.7	28.6 ± 0.7	7.2 ± 0.0	0.39 ± 0.04	1.5 ± 0.4	335 ± 72
Freshwater	ow	0.2 ± 0.0	0.8 ± 0.2	3.3 ± 0.1	6.5 ± 0.1	0.15 ± 0.01	BDL	nm
	pw	2.9 ± 1.7	10.9 ± 1.3	14.4 ± 2.3	4.0 ± 0.1	0.24 ± 0.04	0.6 ± 0.0	109 ± 35

Initial measurements in sediment					
Sediment type	MeHg (ng g^{-1})	MeHg log (K_d [L kg^{-1}])	THg (μg g^{-1})[a]	THg log (K_d [L kg^{-1}])[a]	LOI (%)
Estuarine	7.9 ± 0.8	3.7 ± 0.1	9.6 ± 0.7	4.5 ± 0.1	29% ± 1%
Freshwater	2.3 ± 0.1	3.6 ± 0.0	2.8 ± 0.8	4.4 ± 0.2	13% ± 1%

[a] Note that initial THg sediment levels were not taken. Instead, sediment THg levels reported here (and corresponding KD calculations) reflect the average of all final THg measurements taken for each sediment type. BDL = below detection limits, nm = not measured. Values are reported as the average (of three replicates) plus/minus one standard deviation.

sediment under oxygenated surface water. Water replenishment also served to minimize accumulation of ammonia and replace water loss due to evaporation. Existing surface water was partially drained, leaving about 2 cm of water overlying the sediments, then replaced with the source water to the original volume. Surface water volumes through time are shown in SI Fig. S5.

2.3 Sediment microcosm take down

At the end of the study, passive samplers were removed, and sediments and porewaters were sectioned for direct measurement of MeHg and ancillary parameters. Sediment and porewater profiles were collected at 1 cm intervals for comparison with 0.5 cm resolution PS measurements.

At takedown, overlying water was measured and then carefully siphoned off, leaving about an inch of overlying water to limit surface sediment exposure to the ambient lab air. Overlying water was filtered to 0.45 μm, with Whatman™ glass microfiber GD/X syringe filters (polypropylene housing), collected in 120 mL polyethylene terephthalate glycol (PETG) containers, then either immediately analyzed for sulfide/pH or preserved for other chemical analyses. Passive samplers were then extracted, and sediment particles were gently rinsed off with DI water. The enmeshed PS were then immediately sliced into 0.5 cm segments into horizontal strips (SI Fig. S4) using DI-rinsed shears. Segmented enmeshed PS were individually stored frozen in 15 mL polypropylene centrifuge tubes until distillation for MeHg.

To collect sediments and obtain sufficient porewater volume for analyses, multiple 4 cm diameter sediment cores (SI Fig. S4) were extracted from each microcosm, taking care to avoid areas where the PS and the redox probe were inserted. Cores were processed inside an anaerobic chamber (Coy Laboratory Products, Grass Lake, MI, filled with 95% N_2 and 5% H_2 gas) which continually monitored O_2, and removed O_2 using a Pd catalyst system. The sediment cores were segmented vertically at a 1 cm resolution using a lab-built push-operated core extruder. After the sediment cores were placed on the extruder, any remaining overlying water in the top layer was first pipetted off, and the first cm segment was spooned out using the guides on the cores. The next segments, having less water content and being more solid, were pushed out, using the cm guides on the extruder. Each segment was cut with a smooth plastic blade, which was cleaned between each cut.

Sediment core segments of corresponding depths from each microcosm were pooled into air-tight polypropylene centrifuge bottles and centrifuged at 4000 rpm for 20 min to extract porewater. Overlying porewater was decanted and filtered to 0.45 μm (using Whatman™ glass microfiber GD/X syringe filters) within the anaerobic chamber, and the filtrate was collected in 120 mL PETG containers. Porewater aliquots were either immediately analyzed for sulfide/pH or preserved for future analysis. Because of limited porewater volume, aliquots taken for measurement of anions and aqueous metals were taken at a 2 cm resolution (combining aliquots from two consecutive depth segments), while MeHg, THg, sulfide, pH, and DOC aliquots were taken at a 1 cm resolution. The remaining sediments after centrifugation were lyophilized and stored frozen.

2.4 Analytical methods and sample preservation

Sediment and porewater parameters were chosen based on relationships with MeHg biogeochemistry, including microbial processes and complexation. Sediment THg, MeHg, and loss on ignition (LOI) were measured to obtain sediment characteristics. Dissolved organic carbon (DOC), aqueous chloride, and sulfide were measured to assess MeHg complexation and to track the microbial activity – specifically, activity of potentially Hg-methylating organisms. To assess redox changes with depth—and thereby better indicate the microbial processes driving Hg methylation—we also measured pH, aqueous sulfate, nitrate, elemental sulfur, iron, and manganese.

Aqueous pH and ORP (in overlying water and porewater) were measured directly using an ion-selective electrode (ISE) and an InLab Redox Micro probe (Mettler Toledo), respectively. Aqueous sulfide was preserved in sulfide antioxidant buffer (SAOB)[24] and analyzed by ISE. Dissolved organic carbon was measured using a Shimadzu TOC-L. Sulfate, nitrate, and chloride were measured in aqueous samples *via* ion chromatography (Dionex™ Integrion™ HPIC™ System). Aqueous metal cations, including iron and manganese were measured with an Optima 8300 Inductively Coupled Plasma Optical Emission Spectrometer (ICP-OES). In aqueous samples, passive samplers, and sediments, Hg and MeHg were measured using isotope-dilution modifications of EPA Methods 1631e[25] and EPA Method 1630 (ref. 26) respectively, with dual inductively coupled plasma mass spectrometry (ICP-MS; Agilent 7900) and Cold Vapor Atomic Fluorescence Spectrometry (CVAFS) detection. Detailed analytical methods, including sample preservation, preparation, and QA/QC, are provided in the SI Analytical methods section.

2.5 Statistics

Statistical analyses were performed with JMP Statistical Software Student Edition 18.2.1. Data were log-transformed as needed to improve residual normality and homoscedasticity. Model assumptions were evaluated using visual inspection of residual and Q–Q plots, with Shapiro–Wilk tests used as a supplementary check of residual normality. Reported models met these assumptions.

3 Results & discussion

3.1 Microcosm biogeochemistry

Initial sediment characteristics differed substantially between the two sediment types (Table 1). Estuarine sediments contained about three times higher initial levels of MeHg and THg than freshwater sediments. Estuarine sediments also had higher organic matter content, with roughly 29% LOI compared to ~13% in freshwater sediments. Since the microcosms were constructed at different salinities, estuarine surface water and porewaters contained higher initial levels of sulfate than in

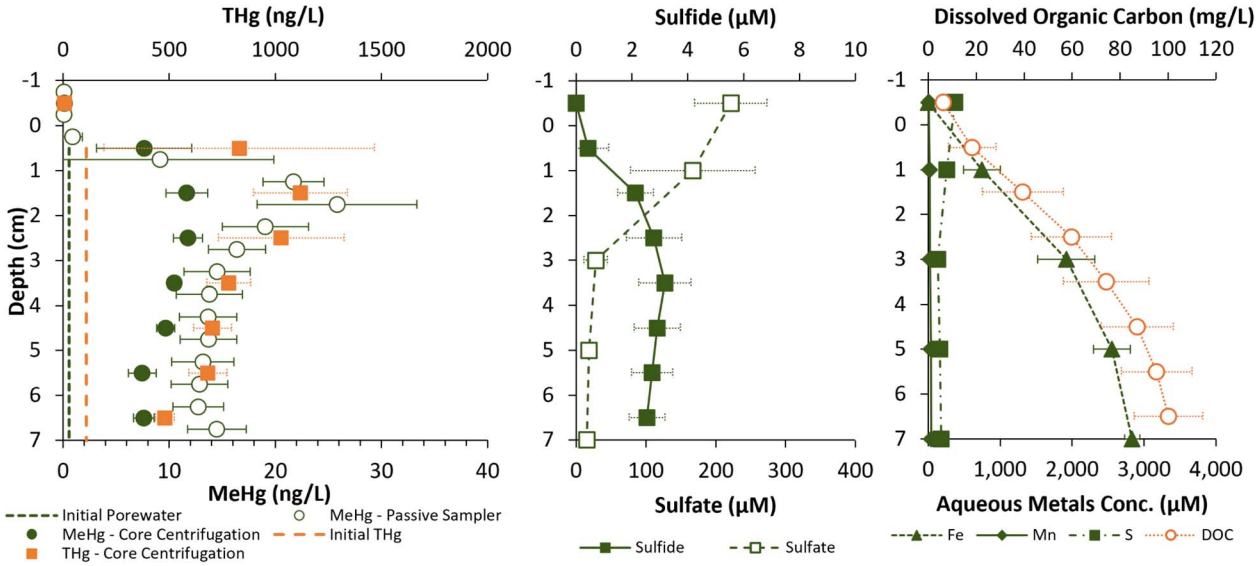

Fig. 1 Porewater profiles for freshwater sediment microcosms at takedown (4 weeks post sampler insertion). Average ($n = 3$) concentrations are plotted with error bars showing one standard deviation. Initial THg and MeHg porewater concentrations are plotted as a vertical dashed line in the left plots. PS-derived aqueous MeHg concentrations are calculated using log $K_{PS} = 2.96$, as per the recommendation by Washburn *et al.* (2022).

freshwater sediments, as intended. The surface water added to the freshwater microcosms contained ~150 μM sulfate and ~20 μM nitrate, while surface water added to estuarine microcosms (made up to be roughly 3 ppt salinity) contained ~1600 μM sulfate and ~270 μM nitrate. Initial porewater sulfate levels of 2900 μM and 4500 μM in the freshwater and estuarine microcosms, respectively, were substantially higher than the overlying water added to microcosms. Porewater chloride levels were also higher, suggesting a contribution from the marsh soils in the sediment mixes. Initial MeHg levels in surface water were below detection limits for both types of microcosms.

Over the 6 week incubation period, both sediment types developed biogeochemical depth gradients indicative of strong microbial activity (Fig. 1 and 2). Surface water remained oxic throughout the experiment (ORP > 190 mV at takedown) due to continuous aeration (SI Fig. S5). Porewater sulfate profiles indicate active sulfate reduction in both sediment types, with maximum depletion at ~3 cm depth in freshwater sediments and ~5 cm in estuarine sediments. Nitrate levels may have supported some denitrification in surficial estuarine sediments, but probably not in the freshwater sediments. Dissolved iron accumulated in both sediments and limited the accumulation

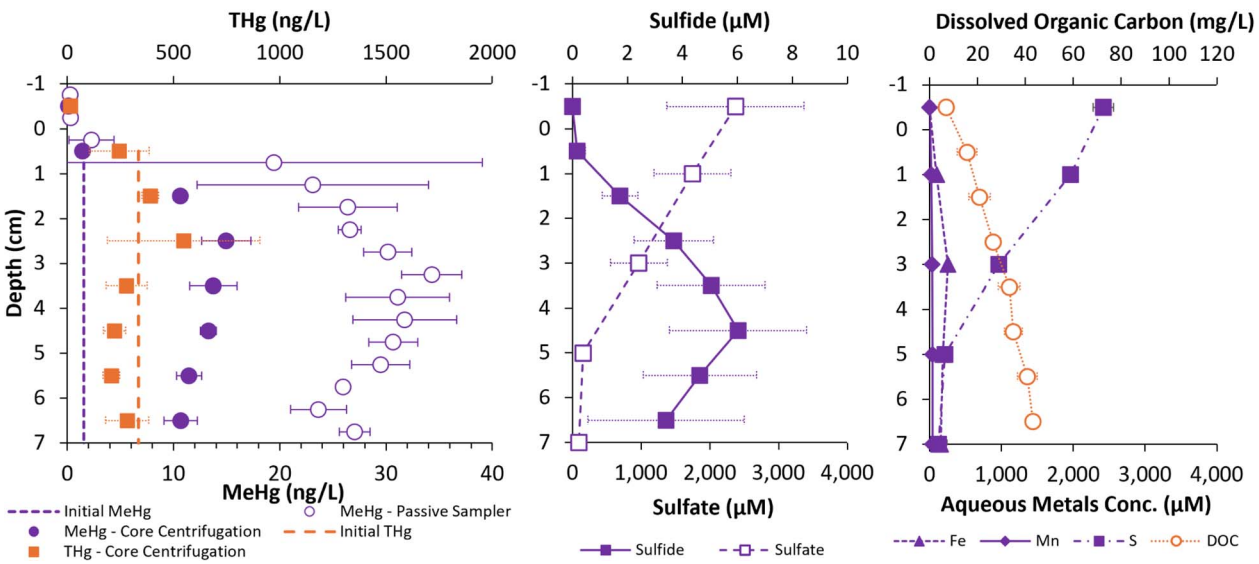

Fig. 2 Porewater profiles for estuarine sediment microcosms at takedown (4 weeks post sampler insertion). Average ($n = 3$) concentrations are plotted with error bars showing one standard deviation. Initial THg and MeHg porewater concentrations are plotted as a vertical dashed line in the left plots. PS-derived aqueous MeHg concentrations are calculated using log $K_{PS} = 2.96$, as per the recommendation by Washburn *et al.* (2022).

of porewater sulfide to a few μM. In freshwater sediments, porewater iron accumulation greatly exceeded sulfate depletion, whereas in estuarine sediments sulfate depletion exceeded iron accumulation.

Sulfate reduction was likely the dominant anaerobic respiratory process in the estuarine sediments, based on molar ratios of electron donors and acceptors, particularly within the 3–5 cm depth zone (SI Fig. S6). In the upper 3 cm, Fe(III) and nitrate reduction were probably active. In the freshwater sediments, dissimilatory Fe(III) reduction appeared to dominate in the top 1–2 cm, with sulfate reduction prevailing below.

Porewater DOC concentrations increased substantially in both sediment types relative to starting concentrations, increasing with depth, indicating strong microbial mineralization of sediment organic matter (Fig. 1 and 2). After the 6 week incubation, DOC increased substantially from initial levels, ranging from an average of 18 mg L^{-1} in the 0–1 cm segment to 100 mg L^{-1} in the 6–7 cm segment in the freshwater microcosms and from 16 mg L^{-1} in the 0–1 cm segment to 43 mg L^{-1} in the 6–7 cm segment in the estuarine sediments. Freshwater sediments showed greater DOC accumulation, reaching higher concentrations than estuarine sediments despite lower initial sediment organic content, suggesting more active microbial degradation of sediment organic matter. In the overlying water, DOC measured 6 mg L^{-1} in freshwater microcosms and 7 mg L^{-1} in estuarine microcosms, an increase from initial values of 2–3 mg L^{-1}.

Microbial activity drove substantial net MeHg production in both types of microcosms, with average sediment MeHg concentrations rising by about a factor of 6 (from 2 to 13 ng g^{-1}) in freshwater sediments and about a factor of 7 (from 8 to 57 ng g^{-1}) in the estuarine sediments (SI Fig. S7). Higher MeHg concentrations in the estuarine sediments reflected higher total Hg concentrations, and possibly higher methylation rates. The fraction of Hg as MeHg at takedown was slightly but significantly higher in the estuarine sediments than in the freshwater sediments (Student's *t*-test, $p < 0.001$). Estuarine sediments averaged 0.60% ± 0.04% Hg as MeHg while freshwater sediments averaged 0.47% ± 0.08%, both across all depths.

After the 6 week incubation, surface water MeHg levels were comparable between the two microcosm types (Fig. 3). Surface water MeHg concentrations were 0.09 ± 0.01 ng L^{-1} in estuarine sediments and 0.13 ± 0.08 ng L^{-1} in the freshwater sediments, although one of the estuarine sediment microcosm replicates was below the detection limit. In estuarine microcosms, surface water THg measured 14.9 ± 4.4 ng L^{-1}, and in freshwater microcosms measured 5.9 ± 1.1 ng L^{-1}.

3.2 Porewater depth profiles in freshwater sediment microcosms

Porewater MeHg was maximal at about 2 cm depth, rising moderately below the sediment–water interface (referred to as SWI throughout) (Fig. 1). Concentrations increased substantially from initial levels of <1 ng L^{-1} at microcosm set-up (Table 1). Average MeHg concentrations in each depth interval (across 3 replicate microcosms) ranged from 7.5 to 11.8 ng L^{-1}. The depth of maximal MeHg corresponded with the zone of maximum sulfate depletion and the transition to more reducing conditions, which is consistent with this being the primary zone of active microbial Hg methylation. Porewater THg also peaked around 2 cm in freshwater microcosms and increased from

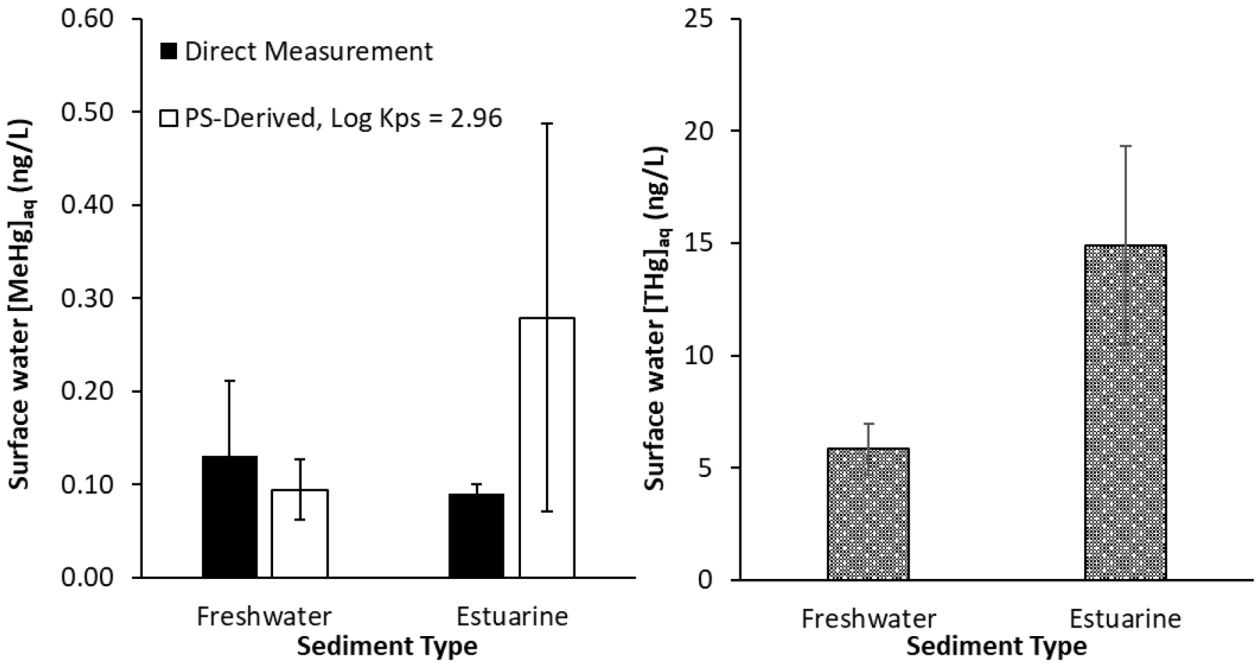

Fig. 3 Surface water MeHg (left) and total Hg (right) concentrations at microcosm takedown (4 weeks post sampler insertion). Passive sampler MeHg estimates were derived using log $K_{PS} = 2.96$ (Washburn *et al.* 2022). For both plots, average ($n = 3$) concentrations are plotted with error bars showing one standard deviation.

initial levels, with depth-specific averages ranging from 161 to 1432 ng L^{-1}. Changes in redox and in DOC concentrations with depth can impact Hg and MeHg porewater concentrations through changes in sediment–water partitioning.

PS-derived MeHg profiles mimicked the shape of direct porewater measurements. MeHg was maximal at the same depth as direct porewater measurements, but with their 0.5 cm resolution, the passive samplers provided more detail in the shape of the profile (Fig. 1). PS-derived MeHg concentrations calculated using the recommended[19] $\log K_{PS} = 2.96$ showed good agreement with direct porewater measurements, falling within a factor of 2 across most depths. Using the ag+AC passive sampler, we were able to observe that the MeHg porewater concentration in the top 0.5 cm of sediment was on average 0.9 ng L^{-1}, and increased sharply by over an order of magnitude to an average of 9.1 ng L^{-1} in the next 0.5 to 1 cm segment. The low MeHg concentrations observed in surface sediments (0–0.5 cm depth) likely reflect lack of production in this zone and diffusive loss to the lower concentration overlying water. This concentration gradient of porewater MeHg concentration in near-surface sediments provides the driving force for MeHg diffusion out of sediments and can be used for the calculation of flux into the overlying water.[27]

3.3 Porewater depth profiles in estuarine sediment microcosms

Estuarine porewaters showed similar depth-dependent patterns to those observed in freshwater sediments, but with the methylation zone shifted deeper into the porewater profile (Fig. 2). Like in the freshwater microcosms, porewater MeHg levels increased over the 6 week incubation; from an initial value or 1.5 ng L^{-1} up to values as high as 15.0 ng L^{-1}. Peak MeHg concentrations occurred at 3–4 cm depth in both PS-derived and direct measurements, corresponding to the deeper zone of sulfate depletion in these higher-sulfate sediments. In estuarine microcosms, porewater THg measurements ranged from 208 to 548 ng L^{-1}, and peaked at 2–3 cm depth, slightly shallower than the MeHg maximum. Porewater THg levels were similar to initial measurements, although they were comparatively elevated at the 2–3 cm depth.

The PS-derived MeHg profiles had a similar shape to direct measurements, but the PS profiles showed a MeHg maxima deeper in the sediments. Using $\log K_{PS} = 2.96$, PS-derived concentrations were generally about a factor of 2–3 above direct measurements.

3.4 Sediment–porewater partitioning

One concern in the use of equilibrium passive samplers is their ability to predict porewater concentrations across different (and perhaps changing) geochemical conditions. In this study, sediment–water MeHg partitioning was quite different between the estuarine and freshwater microcosms and changed over time.

Although initial MeHg partitioning ($\log K_d$), shown in SI Fig. S7, was similar at about 3.7 in both sediments (average across all depths), it dropped over time to an average of 3.2 ± 0.1 at take down in the freshwater sediments, while remaining roughly steady in the estuarine microcosms (3.8 ± 0.3). Partition coefficients for total Hg showed similar patterns, with log K_d in the freshwater sediments decreasing from 4.4 ± 0.2 to 3.6 ± 0.2, while estuarine partitioning stayed about the same (initial $\log K_d = 4.5 \pm 0.1$, final $= 4.6 \pm 0.2$). These differences might reflect higher and increasing porewater DOC in the freshwater sediments, differences in Fe/S chemistry, or other factors. Partition coefficients also changed with depth, especially in the estuarine sediments, where there was much stronger (order of magnitude) partitioning to surface sediments than at depth.

Our goal in measuring partitioning was to evaluate whether the ag+AC samplers could adequately predict porewater MeHg across a range of partitioning behavior. Across the range of K_d values measured in this study (about 1.5 orders of magnitude) the ag+AC PS design was able to predict measured porewater concentrations within a factor of 2–3.

Sediment MeHg concentrations alone do not provide accurate estimates of porewater MeHg concentrations (except roughly across large concentration ranges). Because of the complexity of MeHg biogeochemistry, there is no accepted method to model porewater levels from sediment MeHg concentrations alone.[28,29] Changes in partitioning over time and geochemical conditions as observed here and elsewhere[30] highlight the importance of measuring porewater concentrations directly during sediment assessment.

3.5 Passive sampler performance & applicability across biogeochemical environments

Passive sampler estimations of pore water MeHg concentration provided 0.5 cm depth resolution that is challenging to achieve with direct porewater measurements. Depth profile shapes generally mimicked the shapes of directly measured porewater profiles.

Passive samplers provided roughly the same estimate of error among the three replicates microcosms as did direct porewater MeHg measurements. For measurements made at 0.5 cm intervals, the relative standard deviation (RSD) across the 3 replicate microcosms was ~30% in both freshwater and estuarine sediments. This is comparable to RSDs for the directly measured porewater in this study: 33% for the freshwater and 15% for the estuarine microcosms. For both PS and direct measurement, errors were highest in the top 1 cm depth, likely caused by differences in the development of MeHg profiles at different locations even within the same microcosm (SI Fig. S8) at this sharp redox transition zone.

MeHg concentrations measured by passive samplers ($[MeHg]_{PS}$) were significantly correlated (analysis of variance, $p < 0.001$ for both freshwater and estuarine microcosms) with directly measured surface and porewater MeHg concentrations ($[MeHg]_{aq}$) (Fig. 4). Across both sediment types, porewater MeHg concentrations alone explained 62% of the variability in $[MeHg]_{PS}$. In the freshwater microcosm, median porewater MeHg concentrations predicted by the ag+AC samplers were 1.45 ± 0.56 times the directly measured values, whereas in the

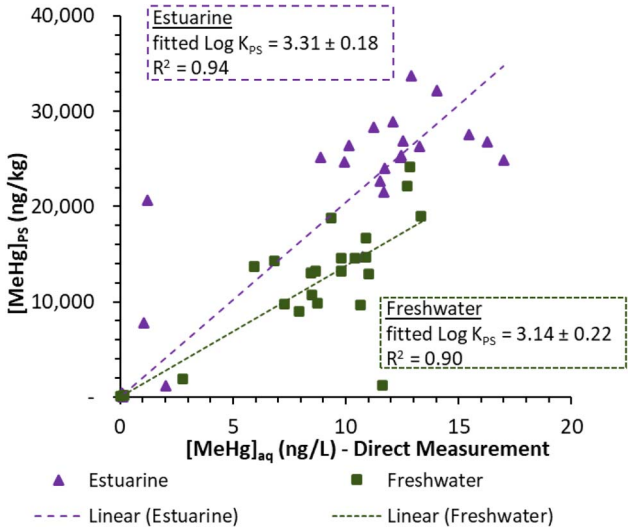

Fig. 4 Relationships between MeHg concentrations in the passive samplers ([MeHg]$_{PS}$, *y* axis) and direct aqueous MeHg measurements in the surface water and porewater ([MeHg]$_{aq}$, *x* axis) for each sediment type. The 0.5 cm passive sampler segments were averaged to consolidate to 1 cm sections to plot against direct porewater measurements (which were sampled at a 1 cm resolution). Modeled linear regressions for untransformed passive sampler MeHg on porewater MeHg. Note that both regressions were forced through zero, as samplers are expected to have zero (or below detection limit) MeHg concentrations in waters with no MeHg (confirmed by blank analysis of PS). Model statistics are as follows: for estuarine microcosms, adjusted $r^2 = 0.93$, on 23 degrees of freedom, $F = 344$, $p < 0.0001$, for freshwater microcosms, adjusted $r^2 = 0.87$ on 23 degrees of freedom, $F = 209$, $p < 0.0001$. Residuals for both models met assumptions of linearity, normality, and homoscedasticity.

estuarine sediments predicted concentrations were higher and more variable (2.3 ± 3.6×). The poorest agreement occurred in the top 1 cm of sediment where concentration gradients were steepest and depth intervals sampled have the greatest impact. Nevertheless, the high correlation coefficients between [MeHg]$_{PS}$ and [MeHg]$_{aq}$ demonstrate that the PS provides reproducible, concentration–proportional responses across the range of porewater MeHg encountered. Plotting [MeHg]$_{PS}$ *versus* [MeHg]$_{aq}$ for each sediment type (Fig. 4) yields an estimated average K_{PS} value for each sediment type across all depths (including surface water). Linear regression yielded a log K_{PS} = 3.14 for freshwater sediments and 3.31 for estuarine sediments. These values are on the high end of the values measured for complexes with natural organic matter (NOM) using laboratory isotherms.[19]

Washburn *et al.*[19] evaluated K_{PS} for MeHg–DOM complexes for our ag+AC samplers using a range of isolated DOM complexes of different character, including humic and fulvic acids and natural organic matter. Organic matter is often the dominant ligand for MeHg in sediment porewaters.[31] Measured log K_{PS} for the tested DOM complexes ranged from ~2.0 to ~3.2, with values for two NOM complexes of 2.8 and 3.2 (SI Table S4). They then tested the samplers in laboratory microcosms, using BCSA sediment mixes similar to those used in this study. After 3 weeks exposure, they found a K_{PS} of ~3.0 provided porewater estimates with a factor of 2 to 4 of directly measured values, about the same accuracy as this study. Using the earlier[19] K_{PS} of $10^{2.96}$ our PS measurements provided porewater MeHg predictions within a factor of 2 for freshwater sediments and 3 for estuarine sediments.

However, to garner confidence in this method and make improvements, it is important to understand the biogeochemical factors that might influence K_{PS} and the accuracy of PS predictions. To do this, we explored how other biogeochemical parameters might help predict MeHg concentration ([MeHg]$_{PS}$) in the passive samplers. To do so, we ran multiple linear regressions on [MeHg]$_{PS}$. Because we have separate sets of variables measured at 1 and 2 cm intervals, we ran models for both sets of data, averaging the 1 cm resolution data across the appropriate intervals for the models that included parameters measured at 2 cm intervals. Parameters were transformed as needed to meet assumptions of homoscedasticity. Overall, porewater MeHg alone explained 62% of the variability in [MeHg]$_{PS}$ in the model for the 1 cm data, with pH explaining an additional 3%. No other parameter (which included DOC, sulfide, [THg]$_{aq}$ and [MeHg]$_{sediment}$) significantly improved the model. For the model of 2 cm intervals data, porewater MeHg explained 65% of variability and SO_4 explained 7% more. Iron, manganese, NO_3, and Cl did not improve the model.

Again, our goal was to evaluate whether the ag+AC samplers could adequately predict porewater MeHg across a range of sediment geochemistry. We found the samplers performed well across a wide range of conditions, including salinity, sulfate, and important MeHg ligands like DOC and sulfide.[19,31–33] To illustrate, Fig. 5 plots surrogate log [MeHg]$_{PS}$/[MeHg]$_{aq}$ in our microcosms *vs.* DOC. Several studies have observed that AC adsorption is depressed in the presence of DOC.[34–36] There was no significant correlation between DOC and log [MeHg]$_{PS}$/[MeHg]$_{aq}$ across both sediment types, although there was a weak but significant correlation for the freshwater microcosms alone ($R^2 = 0.24$, $p = 0.015$). Despite the wide range of DOC concentrations in the freshwater microcosms (5.6 to 110.5 mg L^{-1}), the passive samplers generally predicted measured porewater MeHg concentrations within less that a factor of 2. We conclude that, within the range of conditions in our study, ag+AC samplers are able to predict porewater MeHg concentrations within a readily acceptable range for environmental and remediation studies.

3.6 Environmental implications & future work

Accurate spatial quantification of porewater MeHg is critical for understanding Hg fate and transport and for informing remediation design. Porewater profiling through direct measurement, however, is very challenging in the field, as redox control and sufficient porewater volume are required for a good assessment.[10] Although kinetic and diffusive passive sampling approaches have promise in understanding methylation potential,[37] and exposure risk to benthic and pelagic organisms,[6] the need for site-specific calibration of diffusion rates[12,15] can be a logistical hinderance to some investigations.

The activated carbon-based equilibrium passive sampler (ag+AC) presented here offers an alternative approach to these

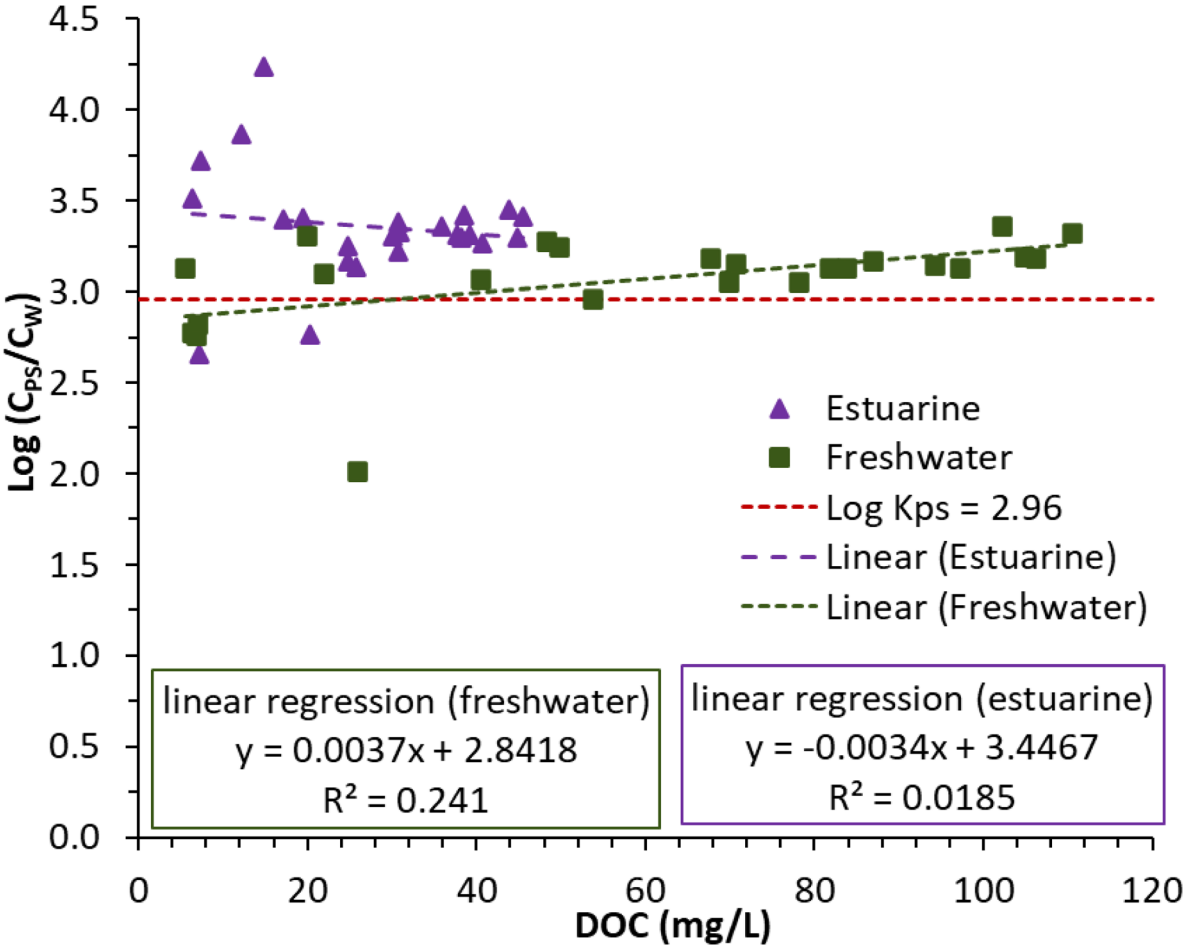

Fig. 5 Relationships between sampler-water partitioning (log C_{PS}/C_{PW}) and porewater dissolved organic carbon (DOC). Data points are averages for each depth (1 cm resolution). Linear regression lines are also plotted, and correlation statistics are shown in the text box. For reference, the recommended sampler-water partitioning (log K_{PS}) from Washburn *et al.* 2022 (log $K_{PS} = 2.96$) is plotted as a horizontal dashed red line. For the freshwater sediment regression, $p = 0.015$, for estuarine $p = 0.53$.

existing methods. These samplers eliminate the need for direct porewater collection and expensive equipment required to maintain redox conditions. Importantly, they can provide more depth resolution than direct measurements, allowing for more accurate assessment of both exposure risk in surface sediments, and MeHg solute efflux across the sediment–water interface. We demonstrated that the samplers accurately predict the shape of directly measured profiles. PS-derived profiles identified depth-resolved MeHg that corresponded with directly measured profiles and with redox transition zones where net methylation is most likely to occur. Identifying the depth of the methylation zone can inform targeted remediation strategies and improve assessments of benthic exposure risk. The fine depth profiling ability can also be used to investigate effects of sediment deposition or performance of remedial caps provided the sampler can be inserted with an appropriate device to the required depth. A finer resolution is possible, when desired, and is only bound by the instrument detection capabilities. A wider sampler cut into finer segments can yield the same mass, therefore same detection capabilities, as the PS samples measured in this study.

In this study, we also continued to evaluate the ability of these samplers to accurately predict porewater MeHg concentrations across a wide variety of environments without the need for additional calibration. We found that measured K_{PS} values were very similar between the estuarine and freshwater sediments tested (freshwater log $K_{PS} = 3.14 \pm 0.227$, estuarine log K_{PS} 3.31 ± 0.18), despite wide ranges in DOC, sulfide and iron in addition to salinity. This demonstrates potential for use in a wide range of environments.

This experiment highlights several points that need to be addressed to gain confidence for use in the field. Although these samplers worked well in these systems, where MeHgDOM is likely the dominant species, these samplers are yet to be tested in environments where MeHgCl or MeHgSH dominates as a species. Testing of these samplers in those environments will improve confidence in this method. Table S4 in the SI provides a list of K_{PS} values previously determined from these samplers, including measurements for specific MeHg complexes in water, and measurements made in natural sediments.

In this study, samplers were inserted by hand, using the marks placed on the sampler as a guide. Due to the high spatial

resolution these samplers offer, exploring tools for a more precise placement are recommended in future deployments, especially *in situ*.

One of the advantages of PS deployed over long time periods (here a month) is that they provide time-integrated estimates of porewater concentrations.[38] In our study, porewater MeHg changed significantly from initial levels. Further, PS—partitioning was slightly higher ($\log C_{PS}/C_W = 3.14$ and 3.31 in freshwater and estuarine microcosms, respectively) than the $\log K_{PS}$ of 2.96 measured previously.[19] Differences in the time course of net MeHg production and partitioning between the freshwater and estuarine microcosms could explain the observed differences in $\log [MeHg]_{PS}/[MeHg]_{aq}$. Additional investigation of PS responses to temporal MeHg variability could help guide sampler deployment strategies.

Conflicts of interest

There are no conflicts to declare.

Data availability

The experimental data for this study are available within the article or its supplementary information (SI). Supplementary information: details of analytical methods used, additional figures of experimental setup and materials used, additional supporting data on water chemistry parameters, tables of data of microcosm experiment details, and excel spreadsheets of all experimental data. See DOI: https://doi.org/10.1039/d5va00492f.

Acknowledgements

The authors acknowledge funding support for this research from the DoD Strategic Environmental Research and Development program (Project ER-2540) and the National Institutes of Environmental Health Sciences, Superfund Research Program (Project # R01ES024284). The Smithsonian Institution also provided support for equipment and facilities. The authors want to thank Steven Brown and the Dow Chemical Company for ongoing support for research on Berry's Creek, and for providing soil samples. At Smithsonian Environmental Research Center (SERC), C. Gionfriddo, A. Soren, C. Pelc, S. Hartnett, and J. T. Bell contributed to experimental and analytical work.

References

1 M. Podar, C. C. Gilmour, C. C. Brandt, A. Soren, S. D. Brown, B. R. Crable, A. V. Palumbo, A. C. Somenahally and D. A. Elias, Global prevalence and distribution of genes and microorganisms involved in mercury methylation, *Sci. Adv.*, 2015, **1**, e1500675.

2 G. N. Bigham, K. J. Murray, Y. Masue-Slowey and E. A. Henry, Biogeochemical controls on methylmercury in soils and sediments: Implications for site management, *Integr. Environ. Assess.*, 2017, **13**, 249–263.

3 C. C. Gilmour, J. T. Bell, A. B. Soren, G. Riedel, G. Riedel, A. D. Kopec and R. A. Bodaly, Distribution and biogeochemical controls on net methylmercury production in Penobscot River marshes and sediment, *Sci. Total Environ.*, 2018, **640–641**, 555–569.

4 K. Ndungu, M. Schaanning and H. F. V. Braaten, Effects of organic matter addition on methylmercury formation in capped and uncapped marine sediments, *Water Res.*, 2016, **103**, 401–407.

5 C. C. Gilmour, T. Bell, A. Soren, G. Riedel, G. Riedel, D. Kopec, D. Bodaly and U. Ghosh, Activated carbon thin-layer placement as an *in situ* mercury remediation tool in a Penobscot River salt marsh, *Sci. Total Environ.*, 2018, **621**, 839–848.

6 A. Amirbahman, D. I. Massey, G. Lotufo, N. Steenhaut, L. E. Brown, J. M. Biedenbach and V. S. Magar, Assessment of mercury bioavailability to benthic macroinvertebrates using diffusive gradients in thin films (DGT), *Environ. Sci. Process. Impacts*, 2013, **15**, 2104–2114.

7 V. F. Taylor, D. Bugge, B. P. Jackson and C. Y. Chen, Pathways of CH3Hg and Hg ingestion in benthic organisms: An enriched isotope approach, *Environ. Sci. Technol.*, 2014, **48**, 5058–5065.

8 J. M. Benoit, D. H. Shull, R. M. Harvey and S. A. Beal, Effect of Bioirrigation on Sediment–Water Exchange of Methylmercury in Boston Harbor, Massachusetts, *Environ. Sci. Technol.*, 2009, **43**, 3669–3674.

9 J. P. Sanders, *A Novel Equilibrium Passive Sampler for Methylmercury and Other Advances in Monitoring and Activated Carbon Remediation for Mercury and PCBs*, University of Maryland, Baltimore County, 2018, DOI: 10.13016/m25b3q-7bsx.

10 R. Mason, N. Bloom, S. Cappellino, G. Gill, J. Benoit and C. Dobbs, Investigation of Porewater Sampling Methods for Mercury and Methylmercury, *Environ. Sci. Technol.*, 1998, **32**, 4031–4040.

11 Y. Hong, N. P. Dan, E. Kim, H. J. Choi and S. Han, Application of diffusive gel-type probes for assessing redox zonation and mercury methylation in the Mekong Delta sediment, *Environ. Sci. Process. Impacts*, 2014, **16**, 1799–1808.

12 S. Noh, Y. S. Hong and S. Han, Application of diffusive gradients in thin films and core centrifugation methods to determine inorganic mercury and monomethylmercury profiles in sediment porewater, *Environ. Toxicol. Chem.*, 2016, **35**, 348–356.

13 M. Zhang, C. Li, X. Ma, L. Yang and S. Ding, Evaluating the mercury distribution and release risks in sediments using high-resolution technology in Nansi Lake, China, *J. Soils Sediments*, 2021, **21**, 3466–3478.

14 C. Gade, L. Mbadugha and G. Paton, Use of diffusive gradient in thin-films (DGTs) to advance environmental mercury research: Development, growth, and tomorrow, *Trends Environ. Anal. Chem.*, 2024, **42**, e00230.

15 C. Fernández-Gómez, J. M. Bayona and S. Díez, Comparison of different types of diffusive gradient in thin film samplers for measurement of dissolved methylmercury in freshwaters, *Talanta*, 2014, **129**, 486–490.

16 G. D. Bland, B. Rao and D. Reible, Evaluating the transport of Hg(II) in the presence of natural organic matter through a diffusive gradient in a thin-film passive sampler, *Sci. Total Environ.*, 2020, **749**, 141217.
17 W. J. G. M. Peijnenburg, P. R. Teasdale, D. Reible, J. Mondon, W. W. Bennett and P. G. C. Campbell, Passive sampling methods for contaminated sediments: State of the science for metals, *Integr. Environ. Assess.*, 2014, **10**, 179–196.
18 J. P. Sanders, A. McBurney, C. C. Gilmour, G. E. Schwartz, S. Washburn, S. B. K. Driscoll, S. S. Brown and U. Ghosh, Development of a Novel Equilibrium Passive Sampling Device for Methylmercury in Sediment and Soil Porewaters, *Environ. Toxicol. Chem.*, 2020, **39**, 323–334.
19 S. J. Washburn, J. Damond, J. P. Sanders, C. C. Gilmour and U. Ghosh, Uptake Mechanisms of a Novel, Activated Carbon-Based Equilibrium Passive Sampler for Estimating Porewater Methylmercury, *Environ. Toxicol. Chem.*, 2022, **41**(9), 2052–2064.
20 S. K. Driscoll, C. C. Gilmour, S. S. Brown, S. Nedrich, G. R. Lotufo, J. D. Farrar, J. A. Steevens, G. Schwartz and J. P. Sanders, Influence of activated carbon on the bioaccumulation of methylmercury from sediment by the amphipod Leptocheirus plumulosus, *Environ. Toxicol. Chem.*, 2025, DOI: 10.1093/etojnl/vgaf259.
21 C. P. J. Mitchell and C. C. Gilmour, Methylmercury production in a Chesapeake Bay salt marsh, *J. Geophys. Res.*, 2008, **113**, DOI: 10.1029/2008jg000765.
22 D. L. Correll, T. E. Jordan and D. E. Weller, Effects of Precipitation, Air Temperature, and Land Use on Organic Carbon Discharges from Rhode River Watersheds, *Water, Air, Soil Pollut.*, 2001, **128**, 139–159.
23 C. C. Gilmour, G. S. Riedel, G. Riedel, S. Kwon, R. Landis, S. S. Brown, C. A. Menzie and U. Ghosh, Activated Carbon Mitigates Mercury and Methylmercury Bioavailability in Contaminated Sediments, *Environ. Sci. Technol.*, 2013, **47**, 13001–13010.
24 H. Brouwer and T. Murphy, Volatile sulfides and their toxicity in freshwater sediments, *Environ. Toxicol. Chem.*, 1995, **14**, 203–208.
25 U.S. Environmental Protection Agency, *Method 1631, Revision E: Mercury in Water by Oxidation, Purge and Trap, and Cold Vapor Atomic Fluorescence Spectrometry*, Office of Water, 2002.
26 U.S. Environmental Protection Agency, *Method 1630. Methyl Mercury in Water by Distillation, Aqueous Ethylation, Purge and Trap, and Cold Vapor Atomic Fluorescence Spectrometry*, Office of Water, 1998.
27 X. Shi, R. P. Mason, M. A. Charette, N. M. Mazrui and P. Cai, Mercury flux from salt marsh sediments: Insights from a comparison between 224Ra/228Th disequilibrium and core incubation methods, *Geochim. Cosmochim. Acta*, 2018, **222**, 569–583.
28 C. S. Eckley, C. C. Gilmour, S. Janssen, T. P. Luxton, P. M. Randall, L. Whalin and C. Austin, The assessment and remediation of mercury contaminated sites: A review of current approaches, *Sci. Total Environ.*, 2020, **707**, 136031.
29 H. Hsu-Kim, C. S. Eckley, D. Achá, X. Feng, C. C. Gilmour, S. Jonsson and C. P. J. Mitchell, Challenges and opportunities for managing aquatic mercury pollution in altered landscapes, *Ambio*, 2018, **47**, 141–169.
30 C. S. Eckley, T. P. Luxton, J. Goetz and J. McKernan, Water-level fluctuations influence sediment porewater chemistry and methylmercury production in a flood-control reservoir, *Environ. Pollut.*, 2017, **222**, 32–41.
31 V. Liem-Nguyen, U. Skyllberg and E. Bjorn, Thermodynamic Modeling of the Solubility and Chemical Speciation of Mercury and Methylmercury Driven by Organic Thiols and Micromolar Sulfide Concentrations in Boreal Wetland Soils, *Environ. Sci. Technol.*, 2017, **51**, 3678–3686.
32 M. Haitzer, G. R. Aiken and J. N. Ryan, Binding of Mercury(II) to Dissolved Organic Matter: The Role of the Mercury-to-DOM Concentration Ratio, *Environ. Sci. Technol.*, 2002, **36**, 3564–3570.
33 U. Skyllberg, Competition among thiols and inorganic sulfides and polysulfides for Hg and MeHg in wetland soils and sediments under suboxic conditions: Illumination of controversies and implications for MeHg net production, *J. Geophys. Res.*, 2008, **113**, DOI: 10.1029/2008JG000745.
34 G. E. Schwartz, J. P. Sanders, A. M. McBurney, S. S. Brown, U. Ghosh and C. C. Gilmour, Impact of dissolved organic matter on mercury and methylmercury sorption to activated carbon in soils: Implications for remediation, *Environ. Sci. Process. Impacts*, 2019, **21**, 485–496.
35 K. A. Muller and S. C. Brooks, Effectiveness of Sorbents to Reduce Mercury Methylation, *Environ. Eng. Sci.*, 2018, **36**, 361–371.
36 C. Chen, Y. Ting, B. L. Ch'ng and H. C. Hsi, Influence of sulfide, chloride and dissolved organic matter on mercury adsorption by activated carbon in aqueous system, *Sustain. Environ. Res.*, 2020, **30**, 22.
37 N. Neal-Walthall, U. Ndu, N. A. Rivera, D. A. Elias and H. Hsu-Kim, Utility of Diffusive Gradient in Thin-Film Passive Samplers for Predicting Mercury Methylation Potential and Bioaccumulation in Freshwater Wetlands, *Environ. Sci. Technol.*, 2022, **56**(3), DOI: 10.1021/acs.est.1c06796.
38 D. W. Hawker, Modeling the response of passive samplers to varying ambient fluid concentrations of organic contaminants, *Environ. Toxicol. Chem.*, 2010, **29**, 591–596.